J Fluoresc (2015) 25:1085–1093
DOI 10.1007/s10895-015-1594-1

ORIGINAL ARTICLE

Spectroscopic Investigation of Interaction Between Carbon Quantum Dots and D-Penicillamine Capped Gold Nanoparticles

Laxman S. Walekar[1] · Samadhan P. Pawar[1] · Uttam R. Kondekar[1] · Dattatray B. Gunjal[1] · Prashant V. Anbhule[1] · Shivajirao R. Patil[1] · Govind B. Kolekar[1]

Received: 23 April 2015 / Accepted: 4 June 2015 / Published online: 26 June 2015

Abstract This study reports the interaction and energy transfer between fluorescent carbon quantum dots (CQDs) and D-Penicillamine capped gold nanoparticles (DPA−AuNPs). The CQDs was synthesized by a simple chemical oxidation method at room temperature. The prepared CQDs shows a strong fluorescence at λ_{em}=430 nm when excited at λ_{ex}=320 nm. The interaction of CQDs with DPA−AuNPs was characterized by fluorescence spectroscopy, Transmission Electron Microscopy (TEM) study and Dynamic Light Scattering (DLS) techniques. The fluorescence study shows the continuous quenching in the fluorescence intensity of CQDs in presence of increasing concentrations of DPA−AuNPs. The change in fluorescence spectra of CQDs in presence of increasing concentration of DPA−AuNPs and quenching are suggestive of a rapid adsorption of CQDs on the surface of DPA−AuNPs. The K_{sv}, K, K_q and n values were calculated and results indicated that the dynamic type of quenching takes place. The distance between donor and acceptor (r) is 6.07 nm which supports the energy transfer by Fluorescence Resonance Energy Transfer (FRET) phenomenon. The plausible mechanism for FRET is also discussed.

Keywords Energy transfer · Fluorescence quenching · Mechanism · Carbon quantum dots · D-Penicillamine · Gold nanoparticles · Interaction study

✉ Govind B. Kolekar
gbkolekar@yahoo.co.in

[1] Fluorescence Spectroscopy Research Laboratory, Department of Chemistry, Shivaji University, Kolhapur 416 004, Maharashtra, India

Introduction

Nowadays, carbon based nanomaterials including carbon quantum dots and carbon nanodots have attracted much attention due to their many novel and unique properties. They were first obtained during the purification of single-walled carbon nanotubes through preparative electrophoresis in 2004 [1], and then via laser ablation of graphite powder and cement in 2006 [2]. Carbon based nanoparticles having a valuable member of nanomaterials due to the abundant and inexpensive nature of carbon [3]. Fluorescent carbon quantum dots becomes one of the best alternative to the traditional fluorophore such as semiconductor quantum dots and organic dyes. They are also referred as carbon nanolights. The fluorescent carbon based carbon quantum dots are superior in terms of their strong aqueous solubility, robust chemical inertness, high resistance to photo bleaching and facile modifications. They also show some biological properties such as low toxicity and good biocompatibility with potential applications in bioimaging, biosensor and drug delivery. The outstanding electronic properties of carbon-based quantum dots as electron donors and acceptors, causing chemiluminescence and electrochemical luminescence, provide them with wide potentials in optronics, catalysis and sensors. The photoinduced electron transfer of CQDs is an interesting property which offers exciting opportunities for light energy conversion, photovoltaic devices and related applications. CQDs can also be used as sensitive nanoprobes for ion detection [4]. The CQDs and nanocomposites were used for the printing ink on the macro/micro scale which is prepared by polymerizing CQDs with certain polymers. Of particular interest and significance is the recent finding that CQDs can exhibit photoluminescence (PL) in the near-infrared (NIR) spectral region under NIR light excitation. It is important that NIR PL emission of CQDs excited by NIR excitation is particularly significant and useful

for in vivo bionanotechnology because of the transparency of body tissues in the NIR "water window" [5].

The strong and tunable luminescence of carbon quantum dots further enhances their versatile properties both fundamentally and technologically [6–9]. In the past few years, various researchers have demonstrated the potential applications of fluorescent CQDs in bioimaging [10–16], light-emitting devices [17], sensors [18, 19], and photovoltaics [20–22]. Compared to conventional quantum dots carbon based fluorescent materials are superior with respect to chemical stability and biocompatibility [23, 24]. Some of the carbon based materials have been reported for their emission in the visible region and hence shows promises in the development of efficient emitters [25]. Many methods have been reported for the synthesis of these environmentally benign carbon nonmaterial's including laser ablation of graphite [25, 26], electrochemical oxidation of graphite [27, 28], electrochemical treatment of multiwalled carbon nanotubes (MWCNTs) [29], chemical oxidation of a suitable precursor [30–38], proton-beam irradiation of nanodiamonds [39, 40], microwave pyrolysis of saccharide [41], and thermal oxidation of suitable precursors [42].

Among these methods, chemical oxidation is effective and convenient synthetic approach for large scale production and it does not require any complex equipment. This method is widely used by many researchers for the preparation of carbon nanoparticles. "Up to now, there have been many attempts to synthesize the various precursors of carbon for the chemical oxidation method. They include, Mustelin et al. [43] and Scrivens et al. [44] isolated CNPs from chemical oxidized arc-discharge single-walled carbon nanotubes (SWCNTs)". The CQDs is also explored as fluorescence resonance energy transfer (FRET) fluorescent sensors to monitor and image analytes (fluorescence microscopy) in living cells as well as in biological processes. From the literature survey, we found that the reports on the FRET between CQDs and metal nanoparticles (MNPs) are limited. Here we have carried out the, FRET study to explore the binding interactions and energy transfer mechanism between CQDs and DPA-AuNPs by spectrofluotometric techniques. Therefore, it is proposed to carry out the interaction study between CQDs and DPA-AuNPs by fluorescence spectroscopy. The different phenomenon like fluorescence quenching, binding mechanism, and energy transfer between donor and acceptor were studied. The values of Stern-Volmer quenching constant (K_{sv}), binding constant (K), number of binding sites (n), distance between donor and acceptor (r) and thermodynamic parameters such as ΔH, ΔS and ΔG were evaluated. The value of r has been determined according to resonance energy transfer. The binding constants at different temperatures were measured according to van't Hoff equation.

In accordance with applying FRET, it was decided to select CQDs as a donor who has well-fluorescence properties with emission at λ_{em}=430 nm and DPA-AuNPs as an acceptor. The absorption spectrum of DPA-AuNPs shows a Surface Plasmon Resonance (SPR) at 520 nm. The slightly overlapping of emission spectrum of CQDs with excitation spectrum of DPA-AuNPs suggested the probability of FRET. The main objective of this present study is to investigate the interaction between CQDs and DPA-AuNPs.

Experimental Section

Equipment

The spectroscopic analysis for the system was carried out using the stable dispersion of nanomaterials. The absorption spectrum was acquired at room temperature on UV Specord, Analytikjena UV–VIS-NIR spectrophotometer with the use of 1.0 cm quartz cell. Fluorescence measurement of solutions were made with PC based Spectrofluorophotometer (JASCO Model FP–8300 Japan) equipped with Xenon lamp source and 1.0 cm quartz cell. Transmission electron microscopy (TEM) images were recorded on a transmission electron microscope (TEM, FEI Tecnai 300). The particle size distribution and Zeta potential of CdS QDs in aqueous suspension was measured by dynamic light scattering (DLS) with a Zetasizer Nano ZS (Malvern Instruments Ltd., UK). The fluorescence life time of CQDs was measured on time resolved fluorescence spectrometer (Horiba's Jobin-Yv on- IBH).

Reagents

All chemical reagents were of analytical reagent grade and used as received without further purification. All aqueous solutions were prepared with doubly distilled water. The metal salt tetrachloro auric acid ($HAuCl_4°8H_2O$) is purchased from S d fine–chem Ltd. (Mumbai, India). The D-Penicillamine (D-PA) was purchased from S d fine–chem Ltd. (Mumbai, India). The stock solution was prepared by dissolving their respective salts in doubly distilled water. Preference was given to use doubly distilled water throughout the experiments.

Synthesis of CQDs

Synthesis of CQDs was carried out via the procedure described by the Z. A. Qiao et al. with some modifications by simple chemical oxidation method [45]. In a typical synthetic procedure, activated wood carbon was used as a source of carbon. The activated wood carbon made available at our laboratory level. Firstly, 0.3 g of activated wood carbon was dispersed in 50 mL of nitric acid (HNO_3) (1 mol/L) aqueous solution and further sonicated for 10 min. The mixture was then refluxed for 12 h. The brownish yellow colored supernatant liquid was formed when cooled to room temperature. The

same solution was neutralized by sodium carbonate (Na_2CO_3), which was further decanted with ethanol and centrifuged at speed of 12,000 rpm results in the formation of solid residue. Then solid residue washed with ethanol and washing was repeated for 4–5 times. The resulting aliquots heated for 5 min. to remove the excess of ethanol which remains concentrated solution of CQDs. This solution was further diluted with double distilled water and stored at 4 °C.

Quantum Yield Measurement

The fluorescence quantum yield of synthesized carbon quantum dots was calculated by using comparative method. Quinine sulfate (literature quantum yield (Φ)=0.54) was used as reference compound. The absolute values were calculated from absorbance and fluorescence intensity of quinine sulfate and CQDs solution at excitation wavelength of 320 nm. The quantum yield of unknown samples was determined by using following equation for comparative method:

$$\Phi = \Phi_R(m/m_R) \times \left(n^2/n_R\right)$$

Where, Φ_R is the quantum yield of reference compound (0.54), m is slope of the line obtained from the plot of integrated fluorescence intensity against absorbance and n is the refractive index of solvent (water, n=1). By putting these values in above equation, we got the fluorescence quantum yield for CQDs (Φ)=0.32.

Results and Discussion

Characterization of Colloidal DPA-AuNPs and CQDs

The DPA capped gold nanoparticles were firstly characterized by UV–vis absorption spectrophotometer and it gives maximum absorption at wavelength of λ_{max}=525 nm as shown in Fig. 1, while synthesized CQDs were characterized by spectrofluorophotometer shows maximum emission at λ_{em}= 430 nm when excited at wavelength of 320 nm (Fig. 2). The particle size of CQDs was measured by using TEM. Figure 3a shows that CQDs are highly dispersed and uniform in aqueous solution, with particle size nearly ranging from 5 to 8 nm.

In addition to that, the particle size measurement of CQDs was also carried out in the aqueous suspension by using DLS experiment. Figure 4a shows the typical size and size distribution of synthesized CQDs by DLS. The average size of CQDs as determined by DLS is 41.7 nm and the size distribution is found within the range 32 to 68 nm, which is considerably larger than the predicted by TEM. This is because; the DLS technique gives us a mean hydrodynamic diameter of CQDs core surrounded by organic layer and solvation layer.

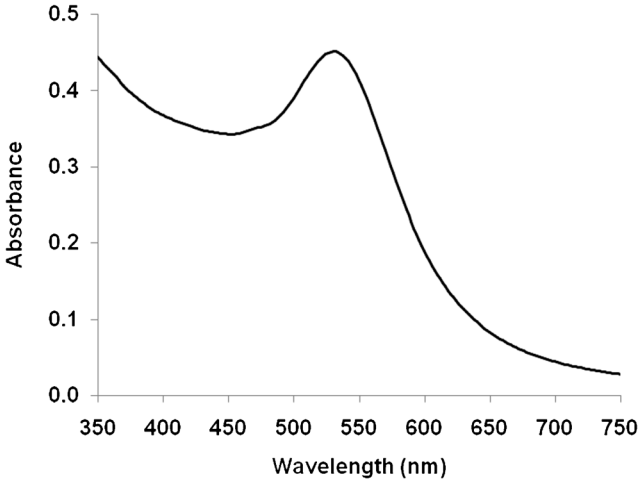

Fig. 1 UV–vis absorption spectum of D-PA capped AuNPs (5×10^{-4} mol L^{-1}) at λ_{max}=525 nm in aqueous colloidal solution

This hydrodynamic diameter is influenced by the viscosity and the concentration of the solution [46].

Fluorescence Quenching Mechanism

Fluorescence quenching phenomenon is one of the powerful tool to provide the information regarding the interaction mode and change in electronic characteristic of nanomaterials. Therefore, the interaction between the CQDs and DPA capped gold nanoparticles was undertaken to study. Generally, the fluorescence quenching is nothing but the decrease in quantum yield of flurophore induced by variety of molecular interaction with quencher molecule [47]. The quenching in fluorescence of fluorophores is mainly attributed to the molecular interaction and many of various processes that takes place with quencher molecule, such as excited state reaction, molecular rearrangement, energy transfer, ground state complex formation, dynamic quenching, inner filter effect etc. It is necessary to make the molecular contact between the fluorophores and quencher for fluorescence quenching. To

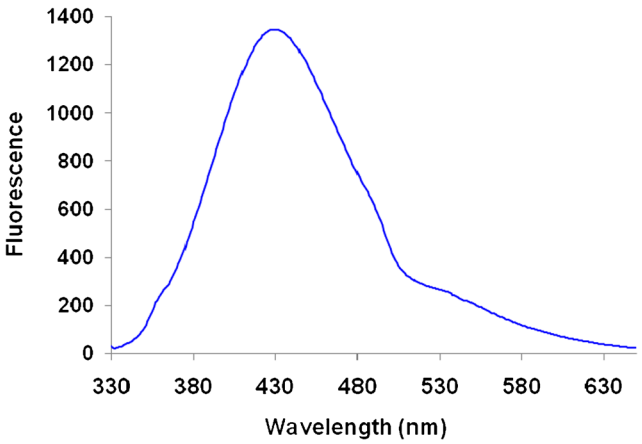

Fig. 2 Fluorescence emission spectrum of CQDs at λ_{exc}=x 320 nm

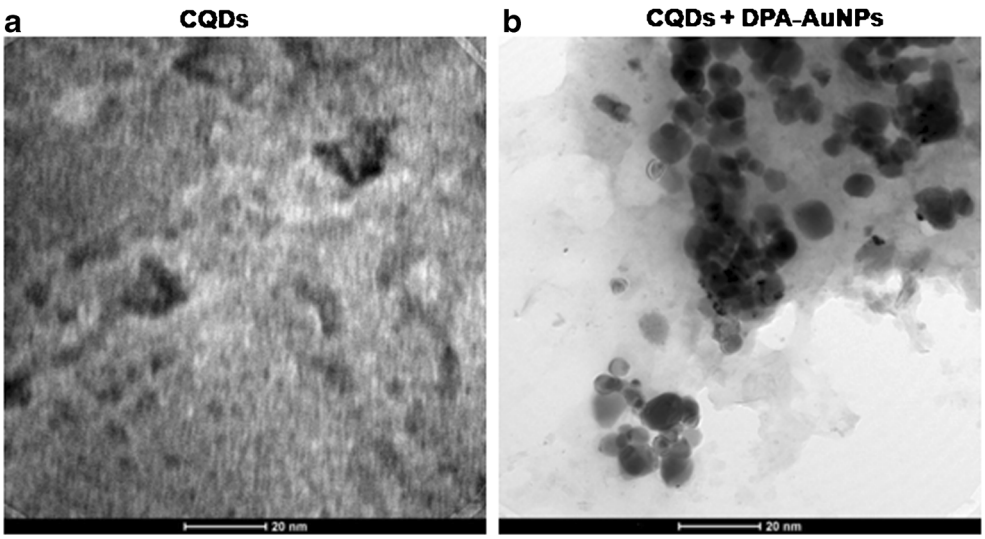

Fig. 3 TEM images of the (**a**) CQDs and (**b**) after addition of DPA-AuNPs (5×10^{-4} mol L^{-1}) added in CQDs colloidal solution

confirm the FRET, we have studied the fluorescence spectra of CQDs in presence of different concentrations of DPA–AuNPs, where we found that the fluorescence intensity goes on decreases gradually with increase in concentration and also increase in temperatures. This suggests as more quencher molecule were added more energy was transferred and more

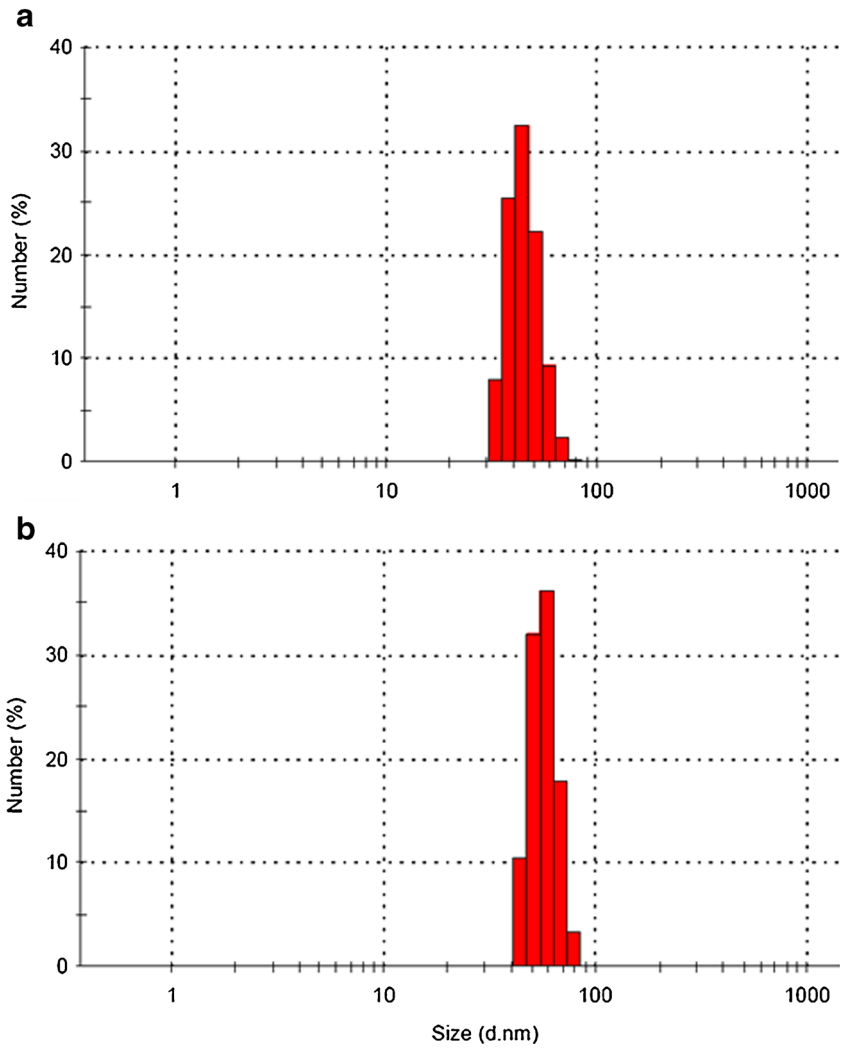

Fig. 4 Size distribution of CQDs measured by DLS varies in response to the addition of DPA-AuNPs (**a**) in the absence of DPA-AuNPs, (**b**) in the presence of (5×10^{-4}) mol L^{-1}.of DPA-AuNPs

adsorption of CQDs with DPA–AuNPs. Figure 5a–d shows the fluorescence spectra of CQDs in the presence of different concentration of DPA capped AuNPs at four different temperature i.e., 299, 304, 309 and 314 K. Previous reports shows that the fluorescence quenching of fluorophore towards the nearby metal nanoparticles could follows the pathways of energy or electron transfer processes [48]. This transfer of energy results in the quenching of fluorescence intensity of CQDs as shown in Fig. 5a–d. A similar type of quenching phenomenon with energy transfer has been observed while studying the photoinduced electron transfer between chlorophyll a and gold nanoparticles [49]. Fig. 6 displays the overlapping of absorption spectra of DPA–AuNPs (curve b) with emission spectra of CQDs (curve a) suggesting of some possibility of energy transfer takes place between them. In our system CQDs acts as donor and DPA–AuNPs acts as acceptor. A change in fluorescence intensity of CQDs upon addition of DPA-AuNPs is a suggestive of interaction and surface adsorption of CQDs with DPA-AuNPs. This quenching in fluorescence is supposed to be attributed to the transfer of energy or transfer of electron takes place between them. Therefore, it is essential to know the type of fluorescence quenching and mechanism of energy transfer. The type of fluorescence quenching was ascribed by the well known Stern-Volmer equation [50, 51].

$$F_0/F = 1 + K_{sv}[Q] \quad (1)$$

$$F_0/F = 1 + K_q\tau_0[Q] \quad (2)$$

Where, F_0 and F are the fluorescence intensity of fluorophores in absence and in presence of quencher respectively. K_{sv}, K_q, [Q] and τ_0 are the Stern-Volmer quenching constant, the quenching rate constant, concentration of quencher and average life time of CQDs in absence of quencher respectively. Figure 7 depicts the Stern-Volmer plot of fluorescence quenching of CQDs with different concentrations of quencher at four different temperatures i. e. 299, 304, 309, 314 K respectively. As per the reports, the plot F_0 / F versus concentration of quencher [Q] should be linear for the quenching type of static or dynamic [52]. The plot showing the good linearity within the investigated concentrations of quencher and agrees with Stern-Volmer equation.

The type of quenching is supposed to be either static or dynamic and can be recognized from the temperature dependence studies. In case of dynamic quenching the K_{sv} values increases with increase in temperature and it decreases with increase in temperature for static quenching [53]. From the K_{sv} values at four different temperature clears that there is dynamic type of quenching takes place between CQDs and DPA-AuNPs (Table 1). The K_{sv} values increases with increase in temperature and the quenching rate constant (K_q) was ~10^{12} $dm^3.mol^{-1}.S^{-1}$. The dynamic type of quenching was also supported by fluorescence life time measurement (Fig. 8). In typical experiment, we have performed fluorescence life time study of fluorophore (CQDs) in aqueous media with and without addition of quencher (DPA-AuNPs). In absence of quencher, the life time of CQDs is 3.64 ns while it falls to 1.98 ns after addition of 5×10^{-4} M of DPA-AuNPs. The decrease in life time of CQDs indicates the excited state reaction between the fluorophore and quencher and hence supports for the dynamic quenching. The fluorescence quenching is attributed to the energy transfer and surface adsorption of CQDs on the DPA-AuNPs surface, which was clearly seen from TEM images as shown in Fig. 3b. Therefore, the fluorescence quenching of CQDs with respect to varying concentrations of DPA-AuNPs was related with the dynamic type of quenching and agrees with experimental results.

Binding Constants and Binding Sites

The binding parameters for the interaction of CQDs with DPA-AuNPs were obtained by using the data of fluorescence quenching studies carried out at four different temperature i.e., 299, 304, 309 and 314 K. The binding parameters includes the binding constant and binding sites (n) and it is calculated by using the following equation,

$$\log[(F_0-F)/F] = \log K + n\log[Q] \quad (3)$$

where, K and n are the binding constants and binding site number respectively. These values were calculated by plotting the graph of $\log[(F_0-F)/F]$ against Log $[Q]$ at four different temperatures, shown in Fig. 9. The Values of binding constant (K) and binding sites (n) were calculated from the intercept and slope which is shown in Table 2 along with regression coefficient R. The results have revealed the presence of a single class of binding sites for CQDs. The binding site values (n) increases with increase in temperatures indicates that the stability of complex between CQDs and DPA-AuNPs goes on strengthening with increase in temperature.

Energy Transfer Between CQDs and DPA-AuNPs

The FRET is an important spectroscopic tool used to investigate a variety of biological phenomenon including energy transfer processes [54]. The FRET is useful to determine the submicroscopic distances between two interactive molecules [55, 56], and to identify active sites in macromolecular assemblies [57, 58]. In the FRET process, an excited donor molecule transfers the excitation energy non radiatively to an acceptor molecule. This process is driven by dipole-dipole interactions between an excited donor molecule (D) and acceptor molecule (A). According to FRET, the rate of energy transfer for dipole-dipole interactions were calculated by $k_{FRET}=(1/d^3)\,(1/d^3)=1/d^6$. The efficiency of energy transfer for FRET phenomenon is strongly depending upon the following three conditions such

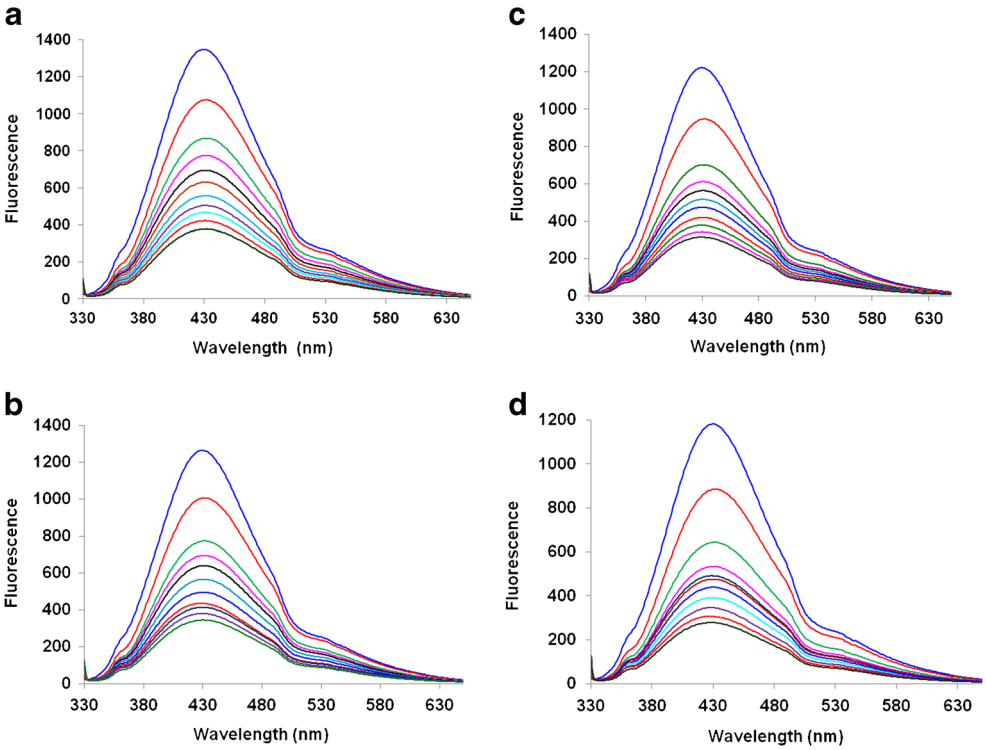

Fig. 5 (**a**), (**b**) (**c**) and (**d**) are the fluorescence spectra of CQDs in presence of DPA-AuNPs at 299, 304, 309 and 314 K temperature respectively. The concentration of DPA-AuNPs (5×10^{-4} mol L^{-1}) from *top to bottom* varies as 0.0, 0.1, 0.2, 0.3, 0.4, 0.5, 0.6, 0.7, 0.8, 0.9, and 1.0 mL

as (a) the extent of overlap of emission spectrum of donor molecule with absorption spectrum of acceptor molecule, (b) distance (r) between the donor and acceptor molecule and (c) the orientation of the transition dipole of donor and the acceptor. In our system, the CQDs acts as a donor and DPA capped AuNPs acts as an acceptor molecule. The efficiency of energy transfer is mainly depend upon the distance between the donor and acceptor molecule (r) and is given by,

$$E = 1-F/F_0 = \frac{R_0^6}{R_0^6 + r^6} \tag{4}$$

where, r is the binding distance between donor and acceptor, and R_0 is the critical distance when probability of efficiency of energy transfer is 50 %. The integral overlap region was used further to calculate the critical energy transfer distance, R_0 and is given by the following Forster relation,

$$R_0^6 = 0.2108\left(\kappa^2\eta^{-4}\phi_D J(\lambda)\right)^{1/6} \quad \left(\text{In A}^0\right) \tag{5}$$

In the above equation, k^2 is the orientation factor which is related with the geometrical orientation of donor and acceptor molecule and k^2 is 2/3 or (0.6667) for the random orientation of molecules in solutions, ή is the refractive index of the medium used, Φ_D is the quantum yield of the donor in the absence of the acceptor and J is spectral overlap integral between the donor

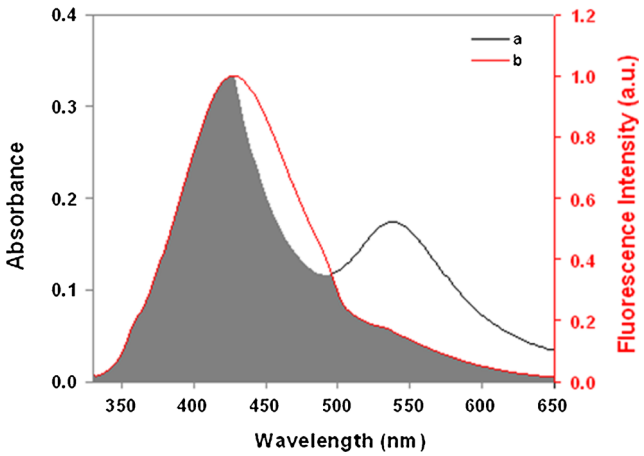

Fig. 6 Overlay plot for absorption spectrum of DPA capped AuNPs (5×10^{-4} mol L^{-1}) and fluorescence spectrum of CQDs

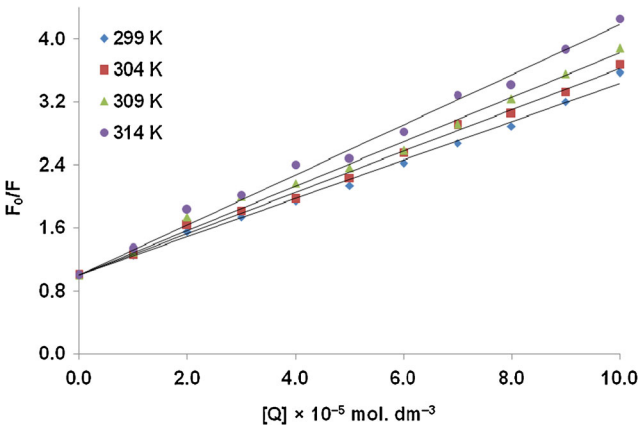

Fig. 7 The Stern–Volmer plots for quenching of CQDs fluorescence by DPA-AuNPs (5×10^{-4} mol L^{-1}) at four different temperatures

Table 1 Stern-Volmer quenching constants and quenching rate constants for interaction between CQDs and DPA-AuNPs at various temperature

T (K)	K_{sv} (X 10^4 $dm^3.mol^{-1}$)	K_q (X 10^{12} $dm^3.mol^{-1}.S^{-1}$)	Correlation coefficient R
299	2.44	6.70	0.994
304	2.62	7.19	0.995
309	2.82	7.74	0.990
314	3.18	8.73	0.990

emission spectrum and the acceptor absorbance spectrum was approximated by the following summation [59].

$$J = \frac{\int_0^\infty F(\lambda)\varepsilon(\lambda)\lambda^4 d\lambda}{\int_0^\infty F(\lambda)d\lambda} \quad (6)$$

Where, F (λ) is the fluorescence intensity of the donor at wavelength λ to λ + Δλ and ε (λ) is the molar absorption coefficient of the acceptor at wavelength λ.

In the present system following values were used to calculate the critical energy transfer distance, R_0. K^2=2/3, = 0.6666, η=1.336 for water and Φ_D=0.32. By putting these values in above equation no. (5), we calculated the E=0.4795, R_0= 5.59 nm, r=6.07 nm and J=5.09×10^{15} cm^{-1} nm^4. The obtained values of distance between donor and acceptor (r) and critical energy transfer distance (R_0) matches with FRET limit of distance within 8 nm. The donor to acceptor distance (r) as well as value of R_0 is less than 8 nm indicates the efficient energy transfer takes place between the donor-acceptor pair [60]. All experimental results are in accordance with predicted by Förster non-radiative energy transfer theory, indicates the energy transfer could be takes place sufficiently from CQDs to DPA-AuNPs which resulting in the quenching in fluorescence of CQDs. It was also suggested that the binding of CQDs to DPA-AuNPs was through energy transfer in accord with dynamic quenching and there should be adsorption of CQDs on surface of AuNPs. The proposed mechanism was also supported by DLS measurement. Particle sizes of CQDs before and after addition of DPA-AuNPs are graphically presented (Fig. 4a and b). The average particle size of CQDs was found to be 41.7 nm (Fig. 4a), on addition of 5×10^{-4} M of DPA-AuNPs, it was enlarged to 62.6 nm (Fig. 4b), showing the tendency toward surface adsorption and this was reflected again in the fluorescence spectra. The quenching in fluorescence of CQDs by DPA-AuNPs due to the surface adsorption and energy transfer was shown in Scheme 1.

Thermodynamic Parameters

Various types of molecular interaction forces exists between the donor molecule and acceptor molecule which include, hydrogen bond, Vander Waals forces, electrostatic and hydrophobic interactions [61]. These forces helps to bind the small molecule with macromolecule. The binding interaction of CQDs with the DPA–AuNPs was influenced by temperature and can be revealed from fluorescence quenching studies as shown in Fig. 5a–d. The temperature dependence binding studies were carried out at four different temperatures i. e. 299, 304, 309 and 314 K. The thermodynamic parameters such as ΔH, ΔS and ΔG were evaluated from the Van't Hoff equation:

$$\ln K = \Delta H/RT + \Delta S/R \quad (7)$$

Where, K is binding constant at corresponding temperature T and R is the gas constant. The enthalpy change (ΔH) and

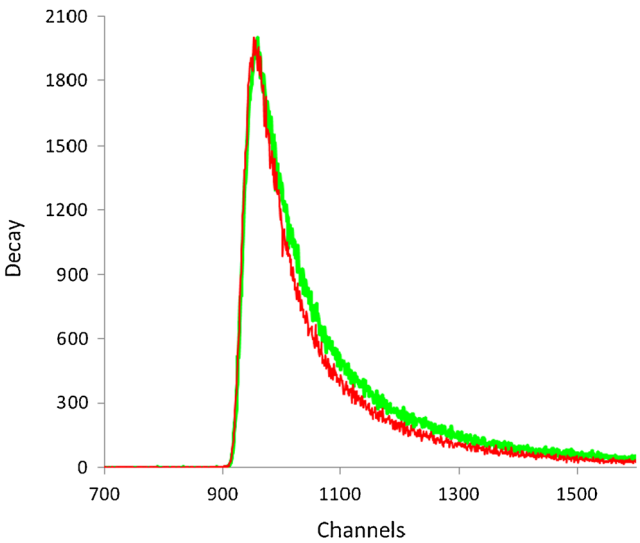

Fig. 8 Fluorescence decay profile of dilute solution of CQDs (curve **A**), and after addition DPA-AuNPs (curve **B**)

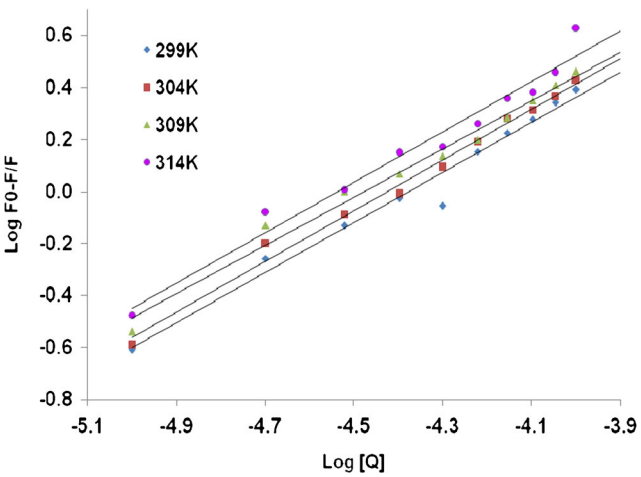

Fig. 9 The plot of log F_0-F/F against log (Q) at four different temperatures

Table 2 Binding constants (K) and number of binding sites (n) of competitive experiment of CQDs–DPA AuNPs system

T (K)	Binding constant K (X 10^4 $dm^3.mol^{-1}$)	Binding sites (n^a)	Correlation coefficient (R)
299	1.89	0.964	0.979
304	2.03	0.970	0.990
309	2.33	0.979	0.970
314	2.57	0.984	0.983

R is the correlation constant

[a] The binding site number (n) approximated to 1

entropy change (ΔS) can be obtained from the slope and the ordinates at the origin of the Van't Hoff plot respectively (Fig. 10). The free energy change (ΔG) can be calculated from the following relationship:

$$\Delta G = \Delta H - T\Delta S \quad (8)$$

These values of ΔH, ΔS and ΔG are calculated and summarized in Table 3. The thermodynamic parameters values indicate that as temperature increases, the binding affinity of CQDs goes on increases towards the DPA-AuNPs which is consistent with endothermic process of binding. The −ve sign of ΔG shows the binding reaction of CQDs with DPA-AuNPs is spontaneous. Endothermic and entropy driven binding events are associated with the hydrophobic effect. It could be suggests that, owing to the binding of CQDs to DPA-AuNPs, some conformational changes were induced consequently enhancing the hydrophobicity between them.

Conclusion

The mechanism of energy transfer and binding interaction between the CQDs and DPA-AuNPs was studied by fluorescence spectroscopy. The emission properties of CQDs were investigated in presence of increasing concentrations

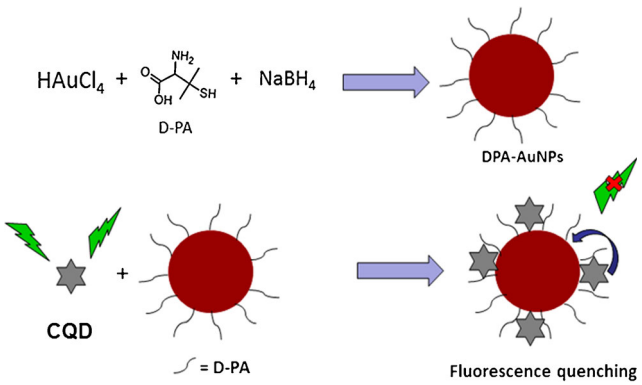

Scheme 1 Schematic presentation for energy transfer from CQDs to DPA-AuNPs

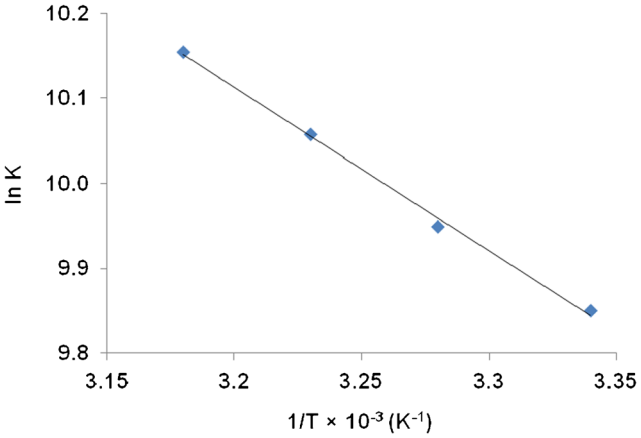

Fig. 10 Van't Hoff plot for the binding interaction between CQDs and DPA-AuNPs

of DPA-AuNPs. It was found that, AuNPs act as strong quencher of CQDs fluorescence and bind with high affinity. The binding process was studied at four different temperatures 299, 304, 309 and 314 K, in addition with this, the Stern-Volmer quenching constant (K_{sv}), the quenching rate constant (K_q) and number of sites (n) were calculated at different temperatures based on the fluorescence quenching data. The Stern-Volmer quenching constant is directly related with the temperatures and it was found that, K_{sv} values goes on increases with increase in temperature strongly supports for the dynamic type of quenching. The binding constant (K) and number of binding sites (n) shows that the CQDs was bound to DPA-AuNPs with approximately one binding sites. The distance between donor and acceptor (r) was 6.07 nm, calculated according to Forster theory supports for the energy transfer takes place between them through FRET phenomenon. The thermodynamic parameters such as ΔS, ΔH and ΔG were evaluated by using the van't Hoff equation. The study of thermodynamic parameters supports the hydrophobic interaction between CQDs and DPA-AuNPs. The fluorescence of CQDs was quenched through the dynamic mode of quenching, and binding between them was mainly based on the hydrophobic force.

Table 3 Thermodynamic parameters of CQDs–DPA AuNPs system at four different temperature

T (K)	ΔH (K J mol^{-1})	ΔG (K J mol^{-1})	x (J mol^{-1} K^{-1})	Correlation coefficient R
299	15.95	−24.44	135.10	0.997
304		−25.11		
309		−25.79		
314		−26.40		

Acknowledgments We are gratefully acknowledging to the UGC, New Delhi for Major research Project (F. No 42-368/2013(SR)), DST-FIST & UGC-SAP, New Delhi for providing funds to our department.

References

1. Xu X, Ray R, Gu Y, Ploehn HJ, Gearheart L, Raker K, Scrivens WA (2004) J Am Chem Soc 126:12736
2. Sun Y-P, Zhou B, Lin Y, Wang W, Fernando KS, Pathak P, Meziani MJ, Harruff BA, Wang X, Wang H (2006) J Am Chem Soc 128: 7756
3. Baker SN, Baker GA (2010) Angew Chem Int Ed 49:6726
4. Haitao L, ZhenhuiKang YL, Shuit-Tong L (2012) J Mater Chem 22:24230
5. Li H, He X, Liu Y, Huang H, Lian S, Lee S-T, Kang Z (2011) CARBON 49:605
6. Iijima S (1991) Nature 354:56
7. Bethune DS, Kiang CH, Devries MS, Gorman G, Savoy R, Beyers R (1993) Nature 363:605
8. Kang ZH, Wang EB, Gao L, Lian SY, Jiang M, Hu CW, Xu L (2003) J Am Chem Soc 125:13652
9. Kang ZH, Wang EB, Mao BD, Su ZM, Gao L, Lian SY, Xu L (2005) J Am Chem Soc 127:6534
10. Sun YP, Zhou B, Lin Y, Wang W, Fernando KA, Pathak P, Meziani MJ, Harruff BA, Wang X, Wang H, Luo PG, Yang H, Kose ME, Chen B, Veca LM, Xie SY (2006) J Am Chem Soc 128:7756
11. Cao L, Wang X, Meziani MJ, Lu F, Wang H, Luo PG, Lin Y, Harruff BA, Veca LM, Murray D, Xie SY, Sun YP (2007) J Am Chem Soc 129:11318
12. Ray S, Saha A, Jana NR, Sarkar R (2009) J Phys Chem C 113:1854
13. Zhu S, Zhang J, Qiao C, Tang S, Li Y, Yuan W, Li B, Tian L, Liu F, Hu R, Gao H, Wei H, Zhang H, Sun H, Yang B (2011) Chem Commun 47:6858
14. Pan DY, Guo L, Zhang JC, Xi C, Xue Q, Huang H, Li JH, Zhang ZW, Yu WJ, Chen ZW, Li Z, Wu MH (2012) J Mater Chem 22: 3314
15. Zhai X, Zhang P, Liu C, Bai T, Li W, Dai L, Liu W (2012) Chem Commun 48:7955
16. Lai CW, Hsiao YH, Peng YK, Chou PT (2012) J Mater Chem 22: 14403
17. Luk CM, Tang LB, Zhang WF, Yu SF, Teng KS, Lau SP (2012) J Mater Chem 22:22378
18. Zhang X, Ming H, Liu R, Han X, Kang Z, Liu Y, Zhang Y (2013) Mater Res Bull 48:790
19. Li Y, Zhang L, Huang J, Liang R, Qiu J (2013) Chem Commun 49: 5180
20. Yan X, Cui X, Li B, Li L (2010) Nano Lett 10:1869
21. Gupta V, Chaudhary N, Srivastava R, Sharma GD, Bhardwaj R, Chand S (2011) J Am Chem Soc 133:9960
22. Li Y, Hu Y, Zhao Y, Shi G, Deng L, Hou Y, Qu L (2011) Adv Mater 23:776
23. Cao L, Wang X, Meziani MJ, Lu FS, Wang HF, Luo PJG, Lin Y, Harruff BA, Veca LM, Murray D, Xie SY, Sun YP (2007) J Am Chem Soc 129:11318
24. Yang ST, Cao L, Luo PGJ, Lu FS, Wang X, Wang HF, Meziani MJ, Liu YF, Qi G, Sun YP (2009) J Am Chem Soc 131:11308
25. Sun YP, Zhou B, Lin Y, Wang W, Fernando KAS, Pathak P, Meziani MJ, Harruff BA, Wang X, Wang HF, Luo PJG, Yang H, Kose ME, Chen BL, Veca LM, Xie SY (2006) J Am Chem Soc 128:7756
26. Hu SL, Niu KY, Sun J, Yang J, Zhao NQ, Du XW (2009) J Mater Chem 19:484
27. Zhao QL, Zhang ZL, Huang BH, Peng J, Zhang M, Pang DW (2008) Chem Commun 5116
28. Zheng LY, Chi YW, Dong YQ, Lin JP, Wang BB (2009) J Am Chem Soc 131:4564
29. Zhou JG, Booker C, Li RY, Zhou XT, Sham TK, Sun XL, Ding ZF (2007) J Am Chem Soc 129:744
30. Bottini M, Balasubramanian C, Dawson MI, Bergamaschi A, Bellucci S, Mustelin T (2006) J Phys Chem B 110:831
31. Xu XY, Ray R, Gu YL, Ploehn HJ, Gearheart L, Raker K, Scrivens WA (2004) J Am Chem Soc 126:12736
32. Liu HP, Ye T, Mao CD (2007) Angew Chem Int Ed 46:6473
33. Tian L, Ghosh D, Chen W, Pradhan S, Chang XJ, Chen SW (2009) Chem Mater 21:2803
34. Peng H, Travas-Sejdic J (2009) Chem Mater 21:5563
35. Liu RL, Wu DQ, Liu SH, Koynov K, Knoll W, Li Q (2009) Angew Chem Int Ed 48:4598
36. Ray SC, Saha A, Jana NR, Sarkar R (2009) J Phys Chem C 113: 18546
37. Zhang JC, Shen WQ, Pan DY, Zhang ZW, Fang YG, Wu MH (2010) New J Chem 34:591
38. Pan DY, Zhang JC, Li Z, Wu MH (2010) Adv Mater 22:734
39. Yu SJ, Kang MW, Chang HC, Chen KM, Yu YC (2005) J Am Chem Soc 127:17604
40. Fu CC, Lee HY, Chen K, Lim TS, Wu HY, Lin PK, Wei PK, Tsao PH, Chang HC, Fann W (2007) Proc Natl Acad Sci U S A 104:727
41. Zhu H, Wang XL, Li YL, Wang ZJ, Yang F, Yang XR (2009) Chem Commun 5118–5120
42. Bourlinos AB, Stassinopoulos A, Anglos D, Zboril R, Georgakilas V, Giannelis EP (2008) Chem Mater 20:4539
43. Bottini M, Balasubramanian C, Dawson MI, Bergamaschi A, Bellucci S, Mustelin T (2006) J Phys Chem B 110:831
44. Xu XY, Ray R, Gu YL, Ploehn HJ, Gearheart L, Raker K, Scrivens WA (2004) J Am Chem Soc 126:12736
45. Qiao ZA, Wang Y, Gao Y, Li H, Dai T, Liu Y, Huo Q (2010) Chem Commun 46:8812
46. Wu YL, Lim CS, Fu S, Tok AIY, Lau HM, Boey FYC, Zeng XT (2007) Nanotechnology 18:215604
47. Lackowicz JR (1999) Principles of fluorescence spectroscopy, 2nd edn. Kluwer Academic/Plenum Publishers, New York
48. George Thomas K, Kamat PV (2003) Acc Chem Res 36:888
49. Barazzouk S, Kamat PV, Hotchandani S (2005) J Phys Chem B 109:716
50. Mote US, Bhattar SL, Patil SR, Kolekar GB (2010) J Lumin 25:1
51. Mokashi VV, Gore AH, Sudarsan V, Rath MC, Han SH, Patil SR, Kolekar GB (2012) J Photochem Photobiol B 113:63
52. Ranjan M, Diffley P, Stephen G, Price D, Walton TJ, Newton RP (2002) Life Sci 71:115
53. Lackowicz JR (1999) Principles of fluorescence spectroscopy, 2nd edn. Kluwer Academic / Plenum Publishers, New York
54. Sklar LA, Hudson BS, Simoni RD (1977) Biochemistry 16:5100
55. Lackowicz JR (2006) Principles of fluorescence spectroscopy, 3rd edn. Springer, New York
56. Stryer L (1978) Annu Rev Biochem 47:819
57. Gorbenko GP, Domanov YAJ (2002) Biochem Biophys Methods 52:45
58. Scholes GD (2003) Annu Rev Phys Chem 54:57
59. Lakowicz JR (2006) Principles of fluorescence spectroscopy, 3rd edn. Springer, New York
60. Zhang YZ, Zhou B, Liu YX, Zhou CX, Ding XL, Liu Y (2008) J Fluoresce 18:109
61. Zhang YZ, Chen XX, Dai J, Zhang XP, Liu YX, Liu Y (2008) Luminescence 23:150